Supporting information

Proton Transport Property in Supported Nafion Nanothin Films by Electrochemical Impedance Spectroscopy.

Devproshad K. Paul[1,2], Richard MacCreery[3] and Kunal Karan[2*]

[1]Dept of Chemical Engineering, Queen's University, Kingston, ON, K7L 3N6, Canada.
[2]Department of Chemical and Petroleum Engineering, University of Calgary, 2500 University Ave., Calgary, AB, T2N 1N4, Canada,
[3]Department of Chemistry, University of Alberta, Alberta, Canada

Corresponding Author: Dr. Kunal Karan E-mail: kkaran@ucalgary.ca (KKaran) Phone-403-220-5754. Fax number: 1-403-284-4852.

The design and fabrication of Interdigitated array (IDA) of Au electrode

For impedance measurement, an IDA of Au electrode supported by SiO_2 (2000 nm)/Si wafer was used as substrate. IDA microelectrode consists of 110 teeth (each teeth is 0.8 cm in length and 10 µm in width) with 100 µm gap between two teeth as shown in Figure S1.

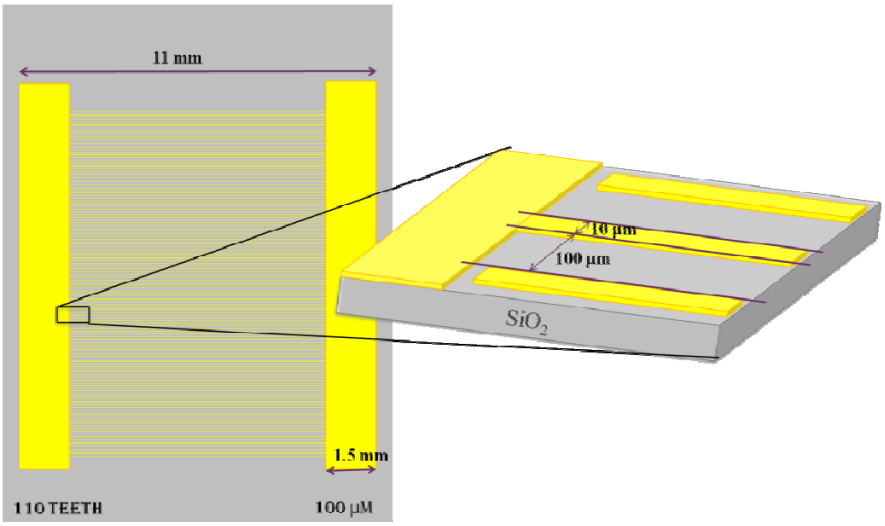

Figure S1: IDA of Au electrode supported by SiO_2 terminated wafer. Gray color represents SiO_2, golden color represents Au electrode. The electrodes were fabricated in the National Institute for Nanotechnology (NINT) lab, Alberta.

Impedance measurement set up and responses

The impedance measurement set up on the IDA electrode system inside the environmental chamber has been presented in Figure S2.

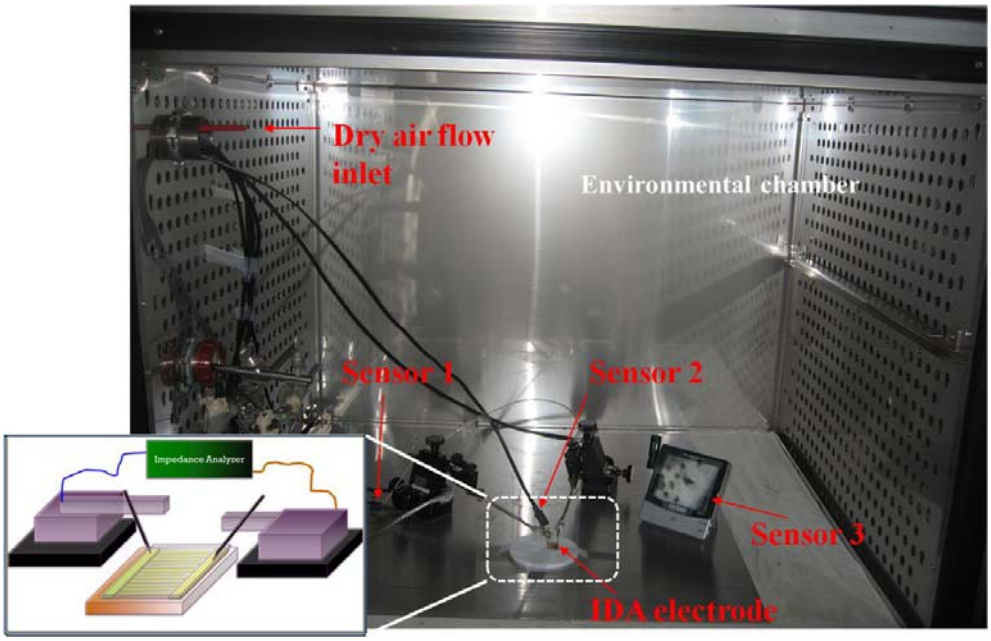

Figure S2: Impedance measurement setup inside the environmental chamber. Nafion® film on IDA of Au electrode has been connected by two probes to the impedance analyzer coupled with dielectric interface.

Below, the impedance response in terms of relative humidity, temperature and film thickness have been presented to visualise and understand which part of the impedance plot can be attributed to film resistance.

Impedance responses at various RH: The impedance responses of 10 nm film for varying RH at 60 ^{o}C have been presented in the Figure S3. The impedance was measured in the frequency ranging from 10 MHz to 0.01 Hz. In each case, the typical impedance response was obtained. While the response pattern was similar, the only observable change was the size of the semi-circle, which decreased with increasing RH.

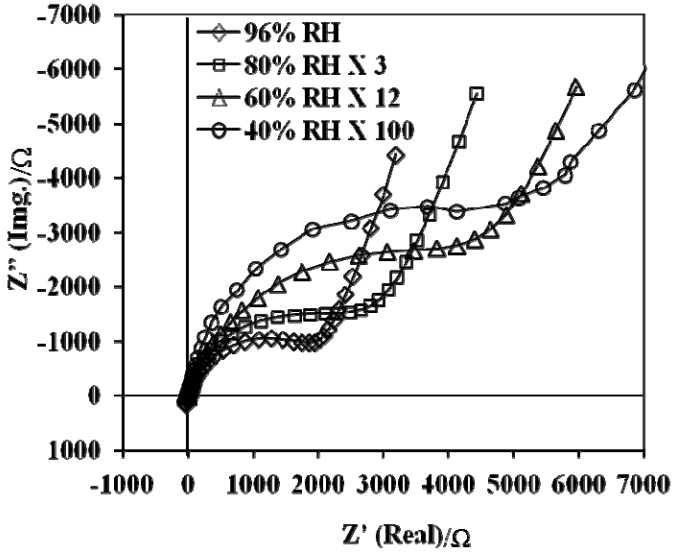

Figure S3: Nyquist impedance plots for 10 nm ultrathin Nafion® film at 60 °C and different RH. The data for 80, 60 and 40% RH have been reduced by 3, 12 and 100 times respectively to fit into the scale.

It is known that the proton conductivity of Nafion® ionomer increases with increasing relative humidity. The decrease in high-frequency resistance with RH is consistent with this observation. Temperature-dependent impedance responses for further confirmation/evidence were also investigated.

Impedance responses for different temperatures: Impedance responses of 55 nm thick film at 80% RH and various temperatures in the 30-60 °C range have been presented in the Figure S4. Similar to RH-dependent impedance responses, major variation was observed in the semi-circle diameter with a variation of temperature. It was found that the resulting semi-circle diameter decreased with increase in temperature from 30 °C to 60 °C. Since Nafion® film conductivity is dependent on temperature, an increase in temperature should result in a decrease in the film resistance. Considering that the semi-circle resistance is due to the film resistance, the observed decrease in semicircle diameter or resistance with increase in temperature is consistent with conductivity behavior of Nafion®.

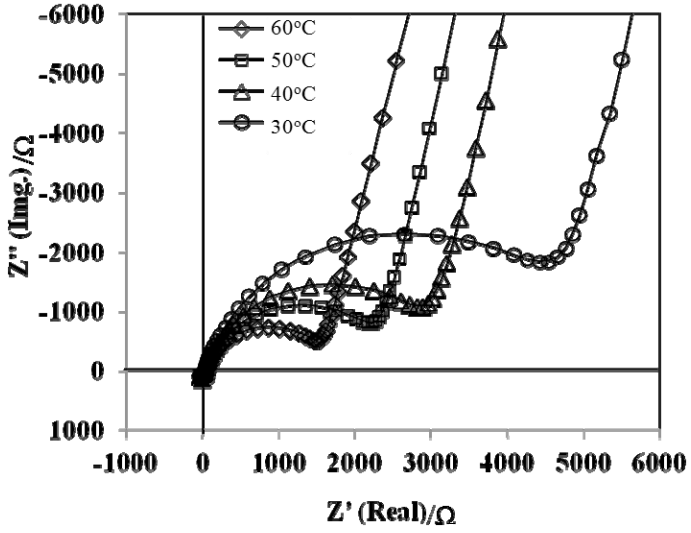

Figure S4: Nyquist impedance plot for 55 nm ultrathin Nafion® film at 80% RH and different temperature.

Impedance responses for nanofilms of various thicknesses: Impedance responses of the thin films with different thicknesses ranging from 4 nm to 300 nm at 60% RH and 60 ^{o}C have been presented in Figure S5. From the impedance responses, it can be noted that the semicircle diameter decreased with increasing thickness. Variation in the shape of the semicircle can also be noted. Interestingly, with decreasing thickness only partial semi-circle can be observed. Compare to the 55 nm and the 300 nm films, the impedance response of the 10 nm film appears distorted. An incomplete semicircle type response was observed for the 4 nm film. The reason of this distorted/incomplete semi-circle response has been discussed later.

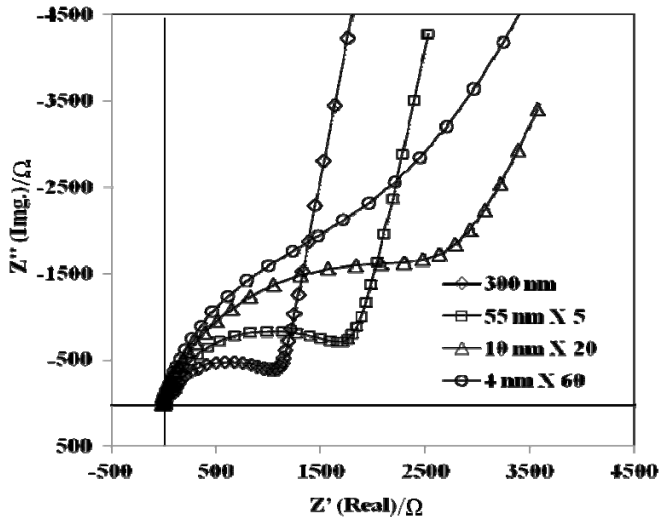

Figure S5: Nyquist impedance plots for ultrathin Nafion® film varying thicknesses at 60% RH and 60 ^{o}C. The data for 55, 10 and 4 nm film have been reduced by 5, 20 and 60 times respectively to fit into the scale.

Impedance responses in different chemical atmosphere: Electrode reactions are expected to occur during ac impedance measurements since proton conduction in the film must be accompanied with the measured external electronic current. The key question is whether the high-frequency semi-circle contains any significant contribution from the interfacial or charge transfer reaction, for example, those arising from oxygen reduction reaction due to exposure of the electrode to air. Impedance measurements in the absence of oxygen were carried out to investigate if electrode reactions contributed significantly to the high-frequency semi-circle response. In this case, a small closed chamber with gas inlet and outlet was used rather than the large environmental chamber. An oxygen sensor along with a RH sensor was placed inside the chamber and the electrode was connected to the impedance measurement set-up. The humidity control for this set of experimental was achieved by bubbling gas (air) through the water but the flow rate was maintained in such a way that 70% RH at room temperature (25 ^{o}C) was achieved. When the external and internal equilibration of the film was established as monitored by the single-frequency impedance measurement protocol, impedance data was collected and termed as the impedance response in O_2 atmosphere. For the impedance measurement in N_2 atmosphere, air was replaced by N_2 gas and passed through the water for half an hour to degas the dissolved oxygen, then the N_2 gas flow through the small chamber. Again the flow was controlled to obtain 70% RH at room temperature. It was confirmed that N_2 has replaced all the O_2 in the chamber as monitored by the oxygen sensor. After equilibration, impedance data was collected – termed as the impedance response in N_2 atmosphere. Similarly, 5% H_2 with argon gas was used for generating 70% RH and oxygen free atmosphere and impedance data was collected – termed as the impedance response in H_2 atmosphere.

The comparative impedance responses for 55 nm film collected in O_2, N_2 and H_2 atmospheres have been presented in the Figure S6. Interestingly, almost identical semicircle responses were observed and the semicircle shape was unhindered even at highly inert N_2 atmosphere. It indicates that the high-frequency impedance response is not generated due to an interfacial oxygen reduction reaction rather attributed due to the film resistance.

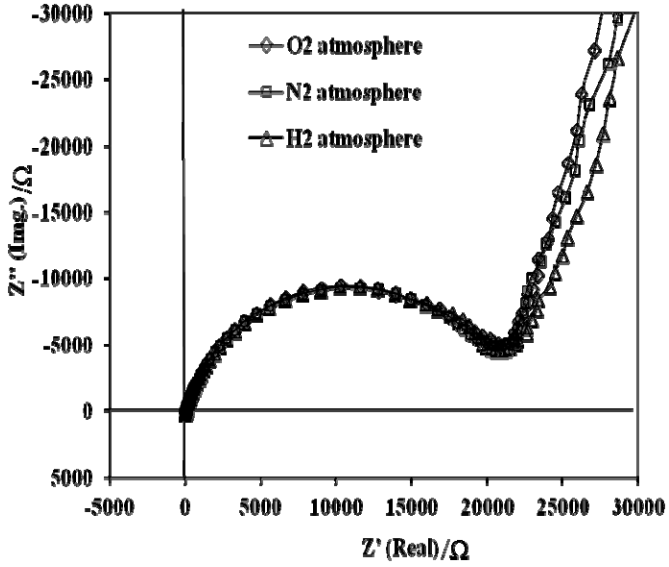

Figure S6: Nyquist impedance plots for 55 nm ultrathin Nafion® film at 25 ºC and 70% RH varying local measurement atmosphere of the film.

Impedance response analysis on the basis of simulation

The shape of the typical semicircle impedance response that varied with the film thickness (as shown in Figure S5) and the possible reasons of incomplete semicircle type of response based on impedance simulation are investigated. In this approach, equivalent circuit, EC-2 (described in the main manuscript) can be expressed as the following equation 2.

$$Z(\omega) = R_s + \frac{1}{(i\omega C_{dl})^{n_{dl}}} + \left[\frac{1}{R_f} + (i\omega C_f)^{n_f}\right]^{-1} \quad (1)$$

where, C_{dl}=*CPE-T*$_{dl}$, n_{dl}=*CPE-P*$_{dl}$, C_f=*CPE-T*$_f$, n_f=*CPE-P*$_f$ have been used for the simplification. Considering the fitting parameters of the previous semicircle, the impedance plot as same as the experimental impedance plot was simulated by using Zview software. In the model fitting results for 55 nm film in Figure S7, double layer capacitance, *CPE-T*$_{dl}$ is two orders of magnitude higher than film capacitance, *CPE-T*$_f$. It was assumed that the incomplete high-frequency arc response might be due to the variation of the capacitance involved in the impedance plot. Therefore, varying *CPE-T*$_{dl}$ but keeping the other circuit elements constant, the impedance response was simulated. When the differences between *CPE-T*$_{dl}$ and *CPE-T*$_f$ became bigger by another one order of magnitude by increasing *CPE-T*$_{dl}$ to 2.6×10^{-06} F, a more complete semicircle was obtained. With further increment of *CPE-T*$_{dl}$ to 2.6×10^{-04} F, a complete semicircle was formed. In contrast, when the *CPE-T*$_{dl}$ was reduced to 2.6×10^{-08} F, the semicircle became incomplete. It is useful to recall that this type of response was observed for the 4 nm film. For *CPE-T*$_{dl}$ of 2.6×10^{-08} F, *CPE-T*$_{dl}$ and *CPE-T*$_f$ became almost similar where no semicircle can be noted for the frequency range examined rather a capacitive response was observed. Expectedly, this indicates that the shape of the impedance response can be determined by the difference between the capacitances. In this particular electrode and Nafion thin film, at least two order of magnitude differences between *CPE-T*$_{dl}$ and *CPE-T*$_f$ should be maintained to achieve apparently, a semicircle type response.

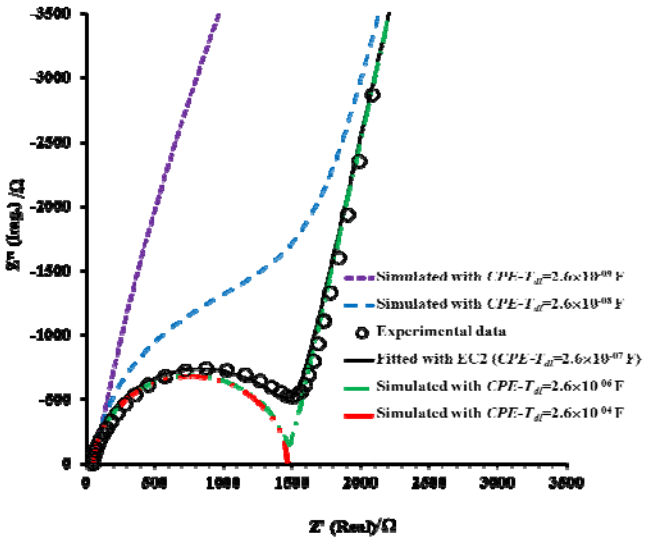

Figure S7: Nyquist plots – experimental data of 55 nm film (open circle), data fitting with EC-2 (solid black line) and simulated data according the EC equation 2 (dotted lines).

To investigate more into the shape of the impedance response, data for the 4 nm film was fitted with EC-2 (*R-CPE$_f$*) as shown in Figure S8. It was found that the incomplete semicircle type response was attributed due to the less difference between *CPE-T$_{dl}$* and *CPE-T$_f$* as presented in Table S1. However, when the impedance was simulated with the same parameters except *CPE-T$_{dl}$* which was considered exactly two order of magnitude different than *CPE-T$_f$* of 1.59×10^{-09} F, the semicircle type response was obtained. Additionally, a complete semicircle response was obtained when a sufficiently high difference between capacitances was considered.

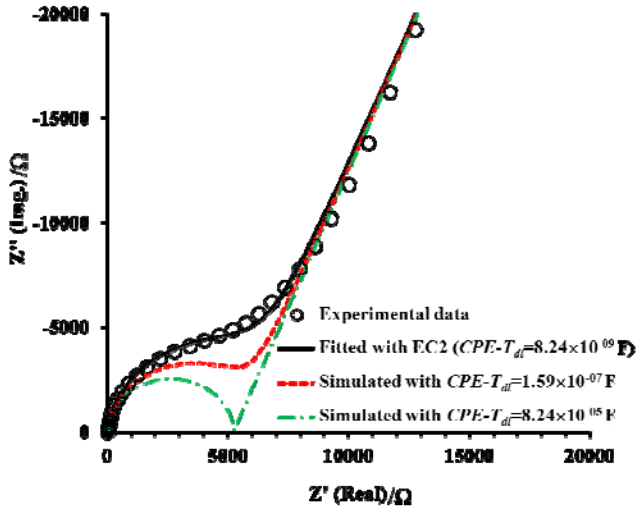

Figure S8: Nyquist plots – experimental data of the 4 nm film (open circle), data fitting with EC-2 (solid black line) and simulated data according the EC equation 5.5 (dotted red and green line).

Table S1: Summarized equivalent circuit fitting parameters with EC-2 for the 4 and 55 nm films.

	55 nm film (at 80% RH)	4 nm film (at 96% RH)
R_S	57.1 Ω	57.4 Ω
C_{dl}=*CPE*-T_{dl}	2.60×10^{-07} F	8.24×10^{-08} F
n_{dl}=*CPE*-P_{dl}	0.87	0.77
R_f	1410 Ω	5196 Ω
C_f=*CPE*-T_f	2.65×10^{-09} F	1.59×10^{-09} F
n_f=*CPE*-P_f	0.98	0.99

n~1would indicate that the film behaves as an ideal capacitor.

Thickness dependent film capacitance at different temperature

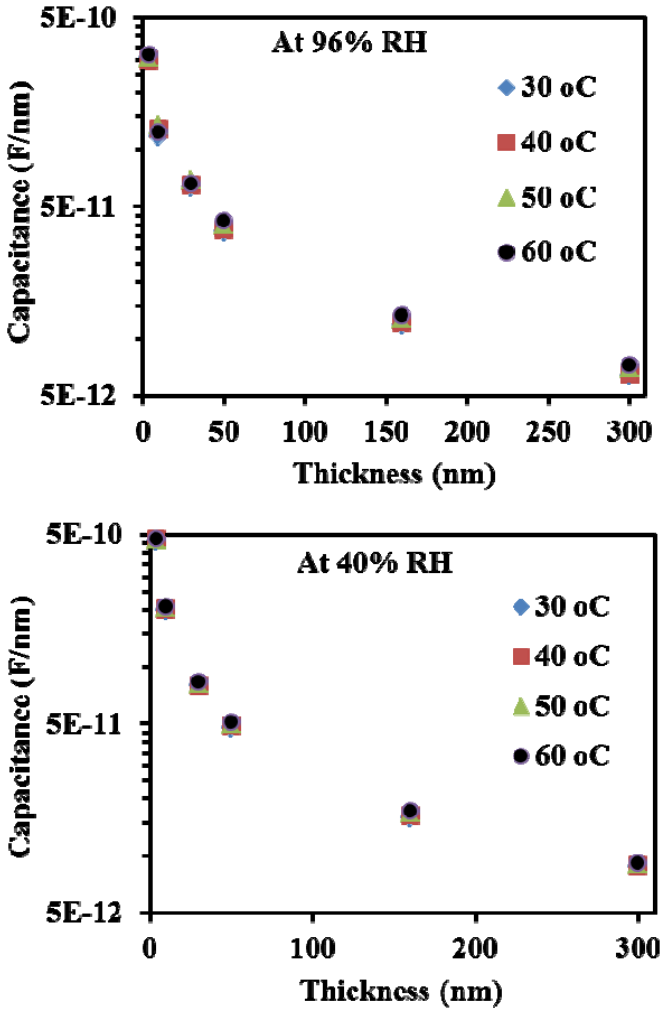

Figure S9: Normalized capacitance of the Nafion® thin films as a function of film thickness for various temperatures (30-60 °C) at 96% RH (Top) and 40% RH (Bottom).

Thickness dependent conductivity data table

Table S2: Proton conductivity data for different films at various RH and 25 ºC

Film thickness	RH	σ (mS.cm^{-1})	Film thickness	RH	σ (mS.cm^{-1})
4 nm	20.50	0.0002	55 nm	20.60	0.0002
	30.30	0.0024		30.45	0.0029
	40.50	0.0206		40.40	0.0269
	59.50	0.4138		59.40	0.5448
	75.60	2.7229		75.20	2.9132
	84.90	7.0973		84.75	7.7854
	95.10	21.888		94.05	22.753
Film thickness	RH	σ (mS.cm^{-1})	Film thickness	RH	σ (mS.cm^{-1})
10 nm	20.80	0.0002	160 nm	20.00	0.3362
	30.20	0.0029		30.00	1.3224
	39.50	0.0199		41.00	3.2505
	50.05	0.1146		51.00	6.0117
	59.35	0.4073		60.00	8.3065
	75.40	2.4823		70.00	13.8568
	85.85	7.8693		81.00	27.0725
	95.00	23.9213		95.00	54.0428
Film thickness	RH	σ (mS.cm^{-1})	Film thickness	RH	σ (mS.cm^{-1})
30 nm	40.00	0.0197	300 nm	20.00	1.5591
	53.00	0.1963		31.00	3.3023
	63.00	0.6528		42.00	8.8389
	79.00	4.1665		53.00	13.6714
	91.00	14.6726		63.00	19.6728
	95.00	23.9051		73.00	29.9814

Table S3: Proton conductivity data for different films at various RH and T

Film thickness (nm)	σ Conductivity (mS.cm^{-1}) at 60 ^{o}C				
	20% RH	40% RH	60% RH	80% RH	95% RH
4	0.003	0.14	1.51	11.16	55.18
10	0.003	0.17	1.72	13.67	62.39
30	0.003	0.16	1.82	16.33	59.78
55	0.007	0.24	2.29	16.60	63.20
160	0.015	0.45	4.31	26.63	93.33
300	0.009	0.44	3.43	26.73	100.60
Film thickness (nm)	σ Conductivity (mS.cm^{-1}) 50 ^{o}C				
	20% RH	40% RH	60% RH	80% RH	95% RH
4	0.001	0.062	1.087	8.335	37.686
10	0.002	0.077	1.031	8.127	57.339
55	0.002	0.121	1.603	9.149	48.934
160	0.007	0.247	2.704	19.221	72.006
300	0.031	1.076	7.185	20.981	83.923
Film thickness (nm)	σ Conductivity (mS.cm^{-1}) 40 ^{o}C				
	20% RH	40% RH	60% RH	80% RH	95% RH
4	0.0003	0.029	0.585	6.164	30.321
10	0.0009	0.034	0.625	5.374	48.799
55	0.0011	0.065	0.931	6.909	40.439
160	0.0032	0.152	1.770	14.162	68.326
300	0.0140	0.605	4.939	17.083	68.334
Film thickness (nm)	σ Conductivity (mS.cm^{-1}) 30 ^{o}C				
	20% RH	40% RH	60% RH	80% RH	95% RH
4	0.0001	0.012	0.278	3.432	21.481
10	0.0003	0.018	0.339	3.895	22.062
55	0.0004	0.028	0.550	4.296	20.185
160	0.0016	0.081	1.120	9.244	34.810
300	0.0071	0.359	2.797	10.978	43.913

Arrhenius plots of the nanofilms with different thickness

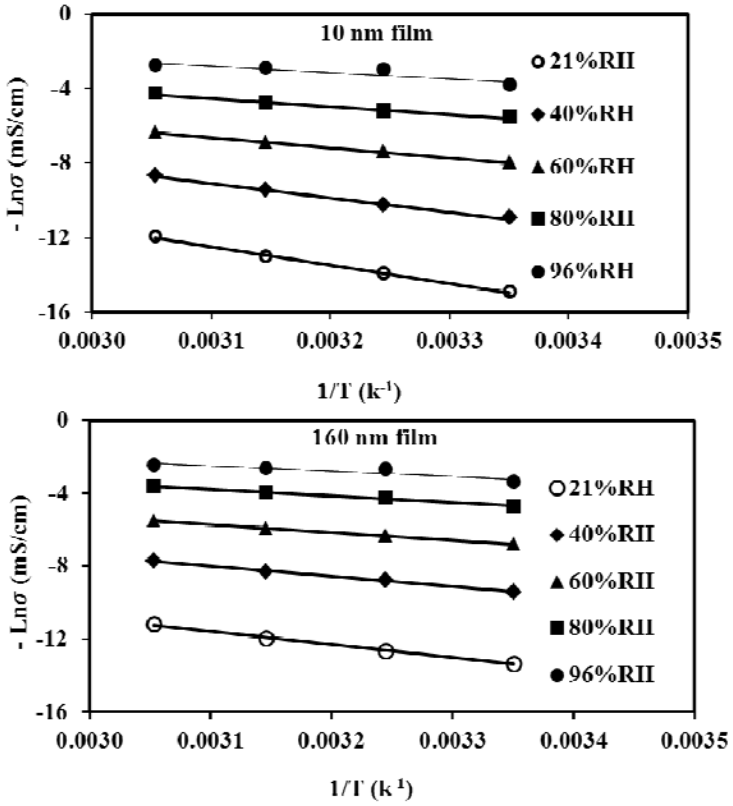

Figure S10: Arrhenius plots for conductivity of the 10 nm and the 160 nm Nafion® thin films.

Activation energy of nanofilms

Table S4: Activation energy data for different films at different RH.

Film thickness (nm)	Activation energy (mJ/cm2)				
	At 20% RH	At 40% RH	At 60% RH	At 80% RH	At 95% RH
4	97.27	67.96	47.10	32.33	25.45
10	82.20	63.52	45.11	34.93	26.83
55	80.00	59.79	48.85	31.92	27.13
160	60.21	46.48	36.33	29.46	23.65
300	60.00	45.00	37.91	30.00	23.40

Effect of inter electrode gap on the proton conductivity of the nanothin films

The proton conductivity of the Nafion® nanofilms was investigated mostly, adopting the Au IDA electrode with the inter-teeth distance 100 µm. At this point, a vital question needs to be answered, whether the proton conductivity of film varied if the inter-teeth distance of Au IDA is less or more than 100 µm. To answer the question, two more IDAs – (i) 30 µm gap and 240 teeth and (ii) 500 µm gap and 24 teeth were adopted for the investigation of 10 nm film conductivity. The film preparation and measurement protocol was as same as that for film prepared IDA electrodes with 100 µm gap. The proton conductivity of the 10 nm film on three different Au IDA electrodes at 60 °C and three different RH has been presented in the Figure S11. It was found that the proton conductivity of the 10 nm film on three IDAs was highly comparable and obtained within 5 to 10% error. Therefore, the difference was acceptable as the results showed up in the sample-to-sample error range.

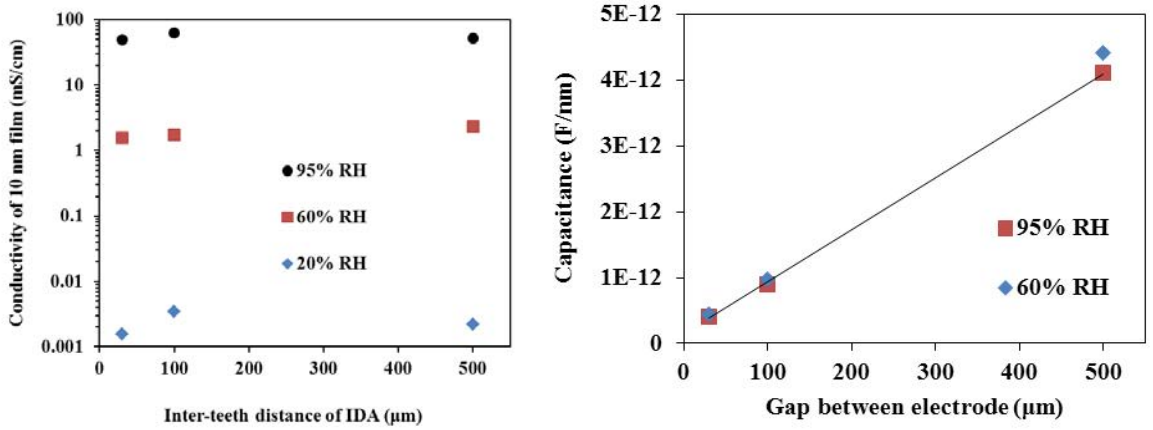

Figure S11: Proton conductivity of the 10 nm film in terms of inter-teeth distance of IDA electrode at 60 °C and three different RH conditions. The normalized capacitance of the 10 nm film in terms of inter-teeth distance of IDA electrode at 60 °C and three different RH conditions.

The capacitance for the 10 nm film was also investigated in terms of inter-teeth distance of IDA. The normalized capacitance has been plotted with inter-teeth distance in the Figure S11 It was found that the normalized capacitance increased with increasing the inter-teeth distances, which fit into a straight line. The linear relationship supports the observed capacitance as film capacitance. However, it is difficult to rule out the cell capacitance contribution to the semicircle.